

Two-flow magnetohydrodynamical jets around young stellar objects

Fabien Casse • Zakaria Meliani • Christophe Sauty

© Springer-Verlag ••••

Abstract We present the first-ever simulations of non-ideal magnetohydrodynamical (MHD) stellar winds coupled with disc-driven jets where the resistive and viscous accretion disc is self-consistently described. The transmagetsonic, collimated MHD outflows are investigated numerically using the VAC code. Our simulations show that the inner outflow is accelerated from the central object hot corona thanks to both the thermal pressure and the Lorentz force. In our framework, the thermal acceleration is sustained by the heating produced by the dissipated magnetic energy due to the turbulence. Conversely, the outflow launched from the resistive accretion disc is mainly accelerated by the magneto-centrifugal force. We also show that when a dense inner stellar wind occurs, the resulting disc-driven jet have a different structure, namely a magnetic structure where poloidal magnetic field lines are more inclined because of the pressure caused by the stellar wind. This modification leads to both an enhanced mass ejection rate in the disc-driven jet and a larger radial extension which is in better agreement with the observations besides being more consistent.

Keywords Winds outflows accretion discs jets YSO galaxies

Fabien Casse

AstroParticule & Cosmologie (APC) 10, rue Alice Domon et Léonie Duquet F-75205 Paris Cedex 13, France

Zakaria Meliani

Institute for Plasma Physics “Rijnhuizen” P.O. Box 1207 NL-3430 BE Nieuwegein, Netherlands

Christophe Sauty

Observatoire de Paris, L.U.Th F-92190 Meudon, France

1 Observational clues

The high velocity of the observed jet in YSOs suggests that they originate from a region that is no larger than one astronomical unity (AU) in extent (Kwan & Tademaru 1988) and between 0.3 to 4.0 AU from the star in the case of the LVC of DG Tau (Anderson et al 2003). This theoretical prediction may be supported for the disc wind by the possible observations of the rotation of several jets associated with TTauris (Coffey et al 2004). Moreover, in the case of Classical TTauris (CTTS) UV observations (Beristain et al 2001; Dupree et al 2005) reveal the presence of a warm wind which temperature is at least of $3 \times 10^5 \text{K}$. It also appears that the source of this wind is restricted to the star itself. These observations are supported by X-ray observations (Feigelson & Montmerle 1999) that reveal the presence in CTTS of hot corona. These observations also suggest the existence of stellar winds in CTTS comparable to the solar wind. These winds may be thermally as well as magneto-centrifugally accelerated.

The aim of the present work is to investigate the formation of two component outflows around YSOs, one coming from the thin accretion disc and the other one being injected from the hot corona of the central star. This work is developed on the base of the disc wind simulations of Casse & Keppens (2002, 2004) (hereafter CK04). The motivation is to study the influence of the stellar wind on the structure and the dynamics of the jet around YSOs.

2 Two-flow jets around YSOs

2.1 MHD simulations set-up

In order to get the evolution of such a disc we solve, by mean of the VAC code designed by Tóth (1996), the

system of time-dependent resistive and viscous MHD equations, namely, the usual conservation of mass, momentum and total energy density e ,

$$e = \frac{\vec{B}^2}{2} + \frac{\rho \vec{v}^2}{2} + \frac{P}{\gamma - 1} + \rho \Phi_G \quad (1)$$

$$\frac{\partial e}{\partial t} + \vec{\nabla} \cdot \left[\vec{v} \left(e + P + \frac{B^2}{2} \right) - \vec{B} \vec{B} \cdot \vec{v} \right] =$$

$$\eta_m \vec{J}^2 - \vec{B} \cdot \left(\vec{\nabla} \times \eta_m \vec{J} \right) - \nabla \cdot \left(\vec{v} \cdot \eta_v \hat{\Pi} \right)$$

where ρ is the plasma density, \vec{v} the velocity, P the thermal pressure, \vec{B} magnetic field and $\vec{J} = \vec{\nabla} \times \vec{B}$ is the current density (provided through the MHD induction equation also solved by the code). The gravitational potential is given by the classical Newton potential generated by a central mass M_* . Note that both resistivity (η_m) and viscosity (η_v) are taken into account in the MHD set of equations. We adopt in our simulations a magnetic Prandtl number $Pr = \frac{\eta_v}{\eta_m} = 1$, believed to be an upper limit of actual Prandtl number in YSO (Lesur & Longaretti 2007). Even with such high value, we have demonstrated that the viscous torque is always much less efficient to remove angular momentum than magnetic torque in thin disks (Meliani et al. 2006). The viscous-resistive disk structure is not modified by the viscous torque as long as the Prandtl number is $Pr \leq 1$. We thus introduce similarly an anomalous viscosity η_v equals to η_m . Through the dependence on the Alfvén velocity in our α prescription (Shakura & Sunyaev 1973), this becomes a profile varying in time and space that essentially vanishes outside the disc. We take $\alpha_m = 0.1$ smaller than one to ensure that the Ohmic dissipation rate at the mid-plane of the accretion disc does not exceed the rate of gravitational energy release (Königl 1995). The initial conditions as well as boundary conditions are fully displayed in Meliani et al. (2006).

2.2 Non-ideal MHD effects in stellar winds

In most stellar wind models, the wind material is often subject to a coronal heating, contributing to the global acceleration of the flow. In our simulations, we assume that the coronal heating is a fraction δ_ϵ of the energy released in the accretion disc at the boundary of the sink region which is transformed into thermal energy in the stellar corona close to the polar axis. This scenario was proposed by (Matt & Pudritz 2005) and is supported by the current observations of hot stellar outflows (Dupree et al 2005). The δ_ϵ parameter range is limited, from below, by the initial thermal acceleration at the surface of the corona which should balance the gravitational force and, from above, the condition to

avoid a too high temperature in the corona (this gives the upper limit). In our simulation we take a small efficient heating corona $\delta_\epsilon = 10^{-5}$. The interaction between the different components of the outflow is responsible for energy dissipation inside the plasma. This energy dissipation is the outcome of non-ideal MHD mechanisms occurring in the wind. In this paragraph, we show how these non-ideal MHD effects are taken into account to prescribe the magnetic resistivity taking place in the wind region in addition to the disc resistivity

$$\eta_m = \alpha_m V_A|_{Z=0} H \exp \left(-2 \frac{Z^2}{H^2} \right) + \alpha_w V_A H_w \exp \left[-2 \left(\frac{R}{H_w} \right)^2 \right]. \quad (2)$$

The first term accounts for the anomalous resistivity occurring in the accretion disc. It vanishes outside the disc ($Z > H$). The second term corresponds to the description of an anomalous resistivity occurring in the outflow close to its polar axis. This term vanishes outside the stellar wind ($R > H_w$) where H_w is the distance from the polar axis where the Alfvén speed encounters a minimum. Hence, the dissipation effects are located in the stellar wind component only and not in the disc wind which is supposed to be less turbulent. For the resistivity in the stellar wind we take $\alpha_w = 10^{-2}$, a lower value than in the disc itself.

2.3 Stellar wind embedded in a disc-driven jet

We first focus on a simulation where the stellar mass loss is set to $10^{-9} M_\odot / yr$. The outcome of our simulation can be seen on Fig. 1 where we have displayed a snapshot of the poloidal cross-section of the structure. In this snapshot we have displayed respectively the density contours (color levels) and the poloidal magnetic field lines (solid lines). The initial accretion disc configuration is close to a hydrostatic equilibrium where the centrifugal force and the total pressure gradient balance the gravity. In the central region, the matter is continuously emitted at the surface of the sink region (designed to be close to the star surface) with sub fast-magnetosonic speed and with a solid rotation velocity profile. Initially, a conical hot outflow (stellar wind) propagates above the inner part of the disc. Its inertia compresses the magnetic field anchored to the accretion disc. As a result the bending of the magnetic surfaces increases, leading to a magnetic pinching of the disc. This pinching delays the jet launching as the disc has to find a new vertical equilibrium. Thus the disc takes a few more inner disc rotations before launching its jet

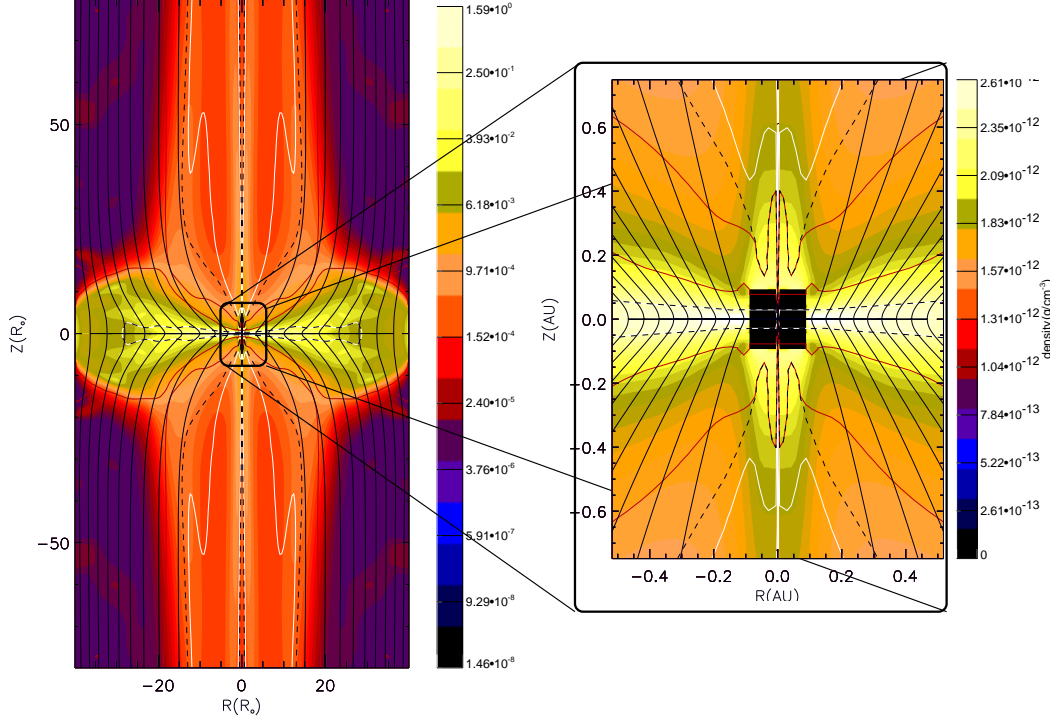


Fig. 1.— Density contours in the poloidal plane of an accretion-ejection structure where a viscous and resistive MHD disc is launching a collimated jet. Magnetic field lines are drawn in black solid lines while the fast magnetosonic surface corresponds the white solid line (Alfvén surface is the black dotted line and slow magnetosonic surface correspond to the red line). A non-ideal stellar wind is emitted from the inner region which ejection mass rate is $\dot{M} = 10^{-9} M_{\odot}/yr$. The disc-driven jet conserves a dynamical structure very similar to the case where no stellar wind is emitted.

compared to CK04. Once the jet has been launched the structure reaches a quasi steady-state where the outflow becomes parallel to the poloidal magnetic field which is parallel to the vertical direction.

The obtained solution is fully consistent with an accretion disc launching plasma with a sub-slowmagnetosonic velocity. The solution crosses the three critical surfaces, namely the slow-magnetosonic, the Alfvén and the fast-magnetosonic surfaces. The other component of the outflow, namely the stellar wind, is injected with sub-fastmagnetosonic velocity and crosses the Alfvén and fastmagnetosonic surfaces. The two components of the outflow become super-fastmagnetosonic before reaching the upper boundary limit of the computational domain. Fig. 1 also shows that the outflow has achieved a quite good collimation within our computational domain. We can distinguish between the two components using the isosurfaces of temperature which are displayed as color surfaces in Fig. 2. In this figure, we can clearly see a hot outflow coming from the central object embedded in the cooler jet arising from the accretion disc.

In order to study the time evolution of both accretion and ejection phenomena in the accretion disc and

around the star, we analyzed the accretion and ejection mass loss rate in both components. Similarly to CK04 we observe a strong increase of the accretion rate in the inner part with time. This behaviour is related to the extraction of the rotational energy of the accretion disc by the magnetic field. Indeed the creation of the toroidal component of the magnetic field in the disc brakes the disc matter so that the centrifugal force decreases leading to an enhanced accretion motion. The mass flux associated with the disc-driven jet slowly increases to reach 18% of the accreted mass rate at the inner radius and contributes to 98% of the total mass loss rate of the outflow. In fact, in this simulation the mass loss rate from the central object is constant ($10^{-9} M_{\odot}/yr$) while the inner accretion rate reaches $10^{-6} M_{\odot}/yr$ and the disc-driven jet mass rate $10^{-7} M_{\odot}/yr$. Hence the stellar outflow does not affect much the overall structure of the outflow. This is confirmed by the shape of the outflow since it is reaching a very similar aspect to the one obtain in CK04 or in the previous simulation without a stellar jet, i.e. a jet confined within 20 inner disc radius.

On Fig. 1, we have displayed density isocontours within

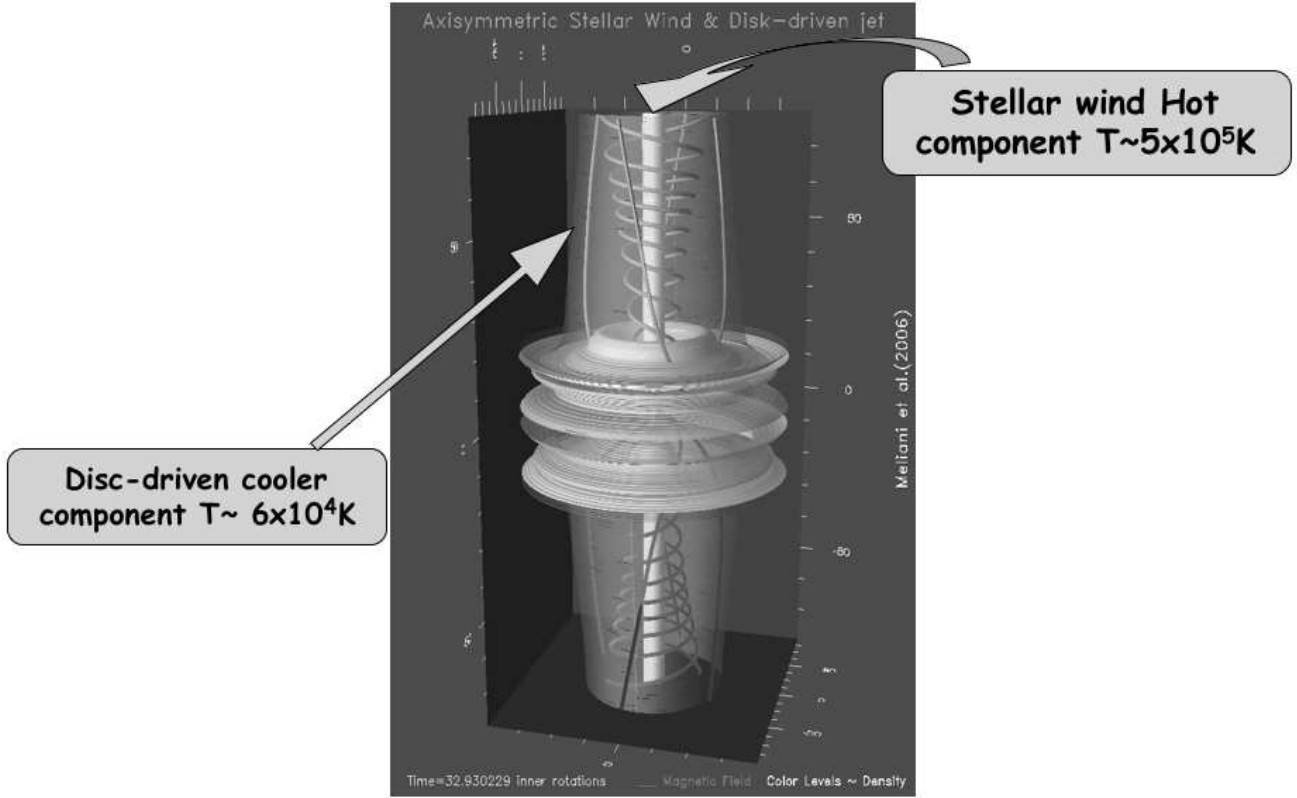


Fig. 2.— Three-dimensional picture of a stellar wind embedded in a accretion disc-driven jet (cf Fig. 1). Colored surfaces stand for temperature levels while green lines represent some magnetic field lines. We clearly see two components arising from this structure: a hot one related to the stellar wind while a more extended cooler one collimates the overall outflow.

a small area around the sink region. Thanks to this plot, we can see that the magnetic lever arm associated with the various outflow components are different. Indeed the disc-driven jet exhibits magnetic lever arm (related to the ratio of the Alfvén radius to the magnetic field line foot-point radius) varying approximately from 9 to 25 while the magnetic lever arm associated with the stellar wind is ranging from 0 near the axis to several tens, if one considered the foot-point of magnetospheric magnetic field line to be anchored to the star. This last magnetic lever arm value may not be very reliable since we have imposed the size of the sink and thus influenced the radial extension of the magnetospheric outflow near the sink. Nevertheless, this simulation illustrates the fact that such large stellar wind magnetic lever arm may be compatible with two-component collimated outflow launched from YSO. This may be the physical mechanism responsible for stellar braking that has to occur in many low-mass stars (see e.g. Matt & Pudritz (2005)). One important issue remains in this model: the amount of thermal energy

released by ohmic heating in the stellar wind is of the order of 35% of the energy released by accretion. One has then to explain how such an amount of energy may be carried away by MHD turbulence to heat the stellar wind. This question remains open.

2.4 Massive stellar winds vs. sun-like mass loss rate wind effects on disc-driven jet

In the simulations presented so far, we have seen that winds with mass loss rate similar to the Sun (up to $10^{-9} M_{\odot}/yr$) do not greatly influence the disc outflow since their general behaviour remains similar. However in the case of a massive stellar jet, the inner wind may strongly influence the outflow as it can be seen in a new simulation performed for a stellar wind mass loss rate set to $10^{-7} M_{\odot}/yr$ (Fig. 3). The radial stellar wind compresses strongly the magnetic field anchored in the accretion disc. The enhanced magnetic field bending (even in the external part of the accretion disc $R > 30$) leads to an increase of the magnetic pinch-

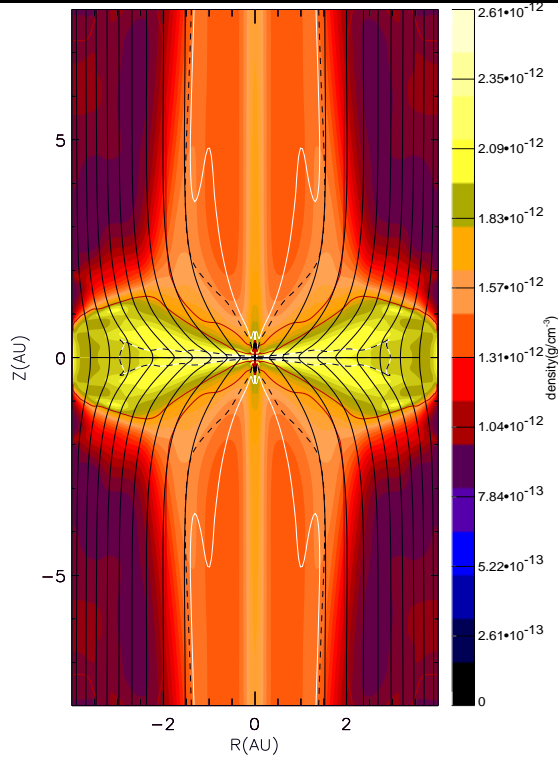


Fig. 3.— Same figure as in Fig. 1 but with a non-ideal stellar wind emitted from the inner region which ejection mass rate $\dot{M} = 10^{-7} M_{\odot}/yr$. The outflow structure is substantially modified by the presence of the stellar outflow since its radial extension is two times larger than in the case with no or weak stellar outflow. The size of the sink region is $R_i = 0.1 AU$ and the stellar mass is $1 M_{\odot}$.

ing in an extended region of the disc $1 < R < 30$. Thus the outflow is launched from all this region since the Blandford & Payne criterion is fulfilled everywhere (Blandford & Payne 1982). Indeed the magnetic field becomes dynamically dominant in the disc corona of this region. The magnetic bending larger than 30° from the vertical direction leads to a centrifugal force and a thermal gradient pressure more efficient to launch the outflow from the disc as it can be seen in the jet mass loss which reached 0.5 of the accretion rate in the inner part.

The angular momentum carried away by the stellar outflow now represents 5% of the accreted angular momentum at the inner radius of the accretion disc. Regarding the acceleration of the outflow, we can distinguish two regions: an internal one corresponding to the contribution from the stellar outflow and an external one coming from the disc-driven jet.

3 Outlook

The present work tried to illustrate the ability of accretion disc-driven jets to focus outflows coming from the central object. We applied MHD simulations to demonstrate this statement in the context of YSOs by self-consistently describing both the accretion disc, its related outflow *and* the wind acceleration. These simulations however left unanswered important question regarding the stellar coronal heating that has to occur in order to give birth to the stellar wind. Another question is the origin of the turbulence warming up the stellar wind as this is also a problem in solar physics.

It is noteworthy that this configuration may be useful in other contexts as for instance in microquasars and AGN. Indeed, when a black hole is the central object of the system, relativistic outflows are believed to arise from its ergosphere (see, e.g. the contribution of J. McKinney in these proceedings). This kind of flow is prone to a substantial decollimating force originating from the displacement current occurring in relativistic MHD regime (Bogovalov & Tsinganos 2005). The collimating action provided by a large-scale non-relativistic disc-driven jet would then be useful to explain the collimation of jets observed in AGN and microquasars.

References

- Anderson, J.M., Li Z.-Y., Krasnopolsky R., Blandford R.D., 2003, ApJL, 590, L107
- Bacciotti F., Ray T. P., Mundt R., Eisloffel J, Solf J., 2002, Ap&SS, 286, 157
- Beristain F. Edwards S., & Kwan J., 2001, ApJ, 551, 1037
- Blandford, R. D., & Payne, D. G. 1982, MNRAS, 199, 883
- Bogovalov S., Tsinganos K., 2005, MNRAS, 357, 918
- Casse F., Keppens R., 2002, ApJ, 581, 988
- Casse F., Keppens R., 2004, ApJ, 601, 90 (CK04)
- Coffey D., Bacciotti F., Woitas J., Ray T. P., Eisloffel, J., 2004, ApJ, 604, 758
- Dupree A. K., Brickhouse N. S., Smith G. H., Strader J., 2005, ApJ, 625, L131
- Feigelson E. D., Montmerle T., 1999, ARA&A, 37, 363
- Königl A., 1995, Rev. Mex. AA., 1, 275
- Kwan J., & Tademaru E., 1988, ApJ, 332, L41
- Lesur, G. & Longaretti, P.Y. 2007, astro-ph/0704.2943
- Matt S., Pudritz R. E., 2005, ApJ, 632, L135
- Meliani Z., Casse F. & Sauty C., 2006, A&A 460, 1
- Shakura N. I., Sunyaev R. A., 1973, A&A, 24, 337
- Tóth, G., 1996, Astrop. Letters & Comm., 34, 245